Coupled Analysis of Ship Motions and Sloshing Flows

Yonghwan KIM
American Bureau of Shipping, Research Department
Houston, TX, USA

1. INTRODUCTION

Ships with liquid cargo experience the slosh-induced internal loads during their operation. In some ships like LNG carriers, the impulsive local load is a major concern for safe structural design, whereas the global forces and moments are of interest in some types of ships. Although the ship motion excites the sloshing flow, the sloshing flow also affects the ship motion in return. Sometimes these slosh-induced forces and moments are significant, so that the coupling effect is critical in the prediction of seakeeping performance for such cases. The anti-rolling tank (ART) is a good example which utilizes this coupling effect. Moreover, the coupling effect between the motion response and fluid flow on deck plays a key role in the dynamic instability problem of small fishing vessels.

This study concentrates on the coupling problem of the ship motions and sloshing flows. In order to solve the coupling problem, two distinct problems - ship motion and sloshing - should be solved at the same time. Generally, the sloshing phenomena in the tank or the deck are strongly nonlinear, so that the time-domain approach seems the right way to tackle. In this study, the finite difference method has been applied to solve the sloshing problem. Particularly, this study adopts the same scheme with [1] and [2]. For the ship motion problem, the Large Amplitude Motion Program (LAMP) has been used. Two programs have been combined, so that the slosh-induced moment affects the ship motion in waves, and vice versa.

The test models are a modified S175 hull equipped with rectangular anti-rolling tanks of passive type and a VLCC with 17 oil tanks. The computational results for the anti-rolling tanks have been compared with experimental data for a supply vessel with the same beam-length and draft-length ratios. The present method is directly applicable to the design of ARTs and sloshing analysis in LNG carriers and FPSOs.

2. BACKGROUND

Consider a freely floating ship equipped with a partially-filled tank. Two Cartesian coordinate systems are defined at the center of ship motion and the tank bottom, as shown in Figure 1. The ship is in the 6-D.O.F. motion which is excited by the incident wave and also the internal forces and moments due to sloshing. The equation of the ship motion can be written as follows:

$$[\mathrm{M}_{ij}]\frac{\partial^2 \vec{\xi}}{\partial t^2}+[\mathrm{B}_{ij}]\frac{\partial \vec{\xi}}{\partial t}+[\mathrm{C}_{ij}]\vec{\xi}=\vec{F}_{ext}(t)+\vec{F}_{slosh}(t) \tag{1}$$

where $\vec{\xi}$ is the displacement of ship motion and $[\mathrm{M}_{ij}]$, $[\mathrm{B}_{ij}]$ and $[\mathrm{C}_{ij}]$ represent the matrices of mass, damping and restoring coefficients. The external excitation force vector $\vec{F}_{ext}(t)$ includes all the forces on the external hull surface by incident waves and hydrodynamic reactions. Moreover, $\vec{F}_{slosh}(t)$, the slosh-induced component, contributes to the excitation. In the present study, the ship motion problem has been considered in the realm of linear theory. Therefore, the linear surface conditions as well as the body boundary condition have been considered in the boundary value problem for the ship motion.

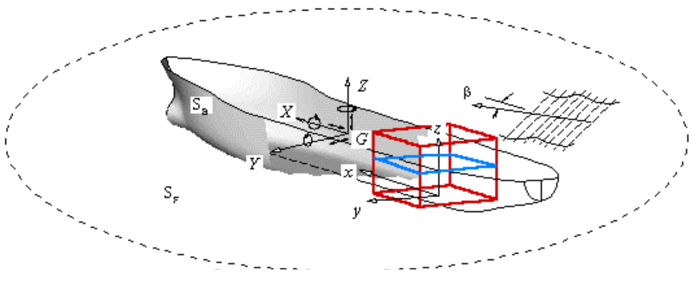

Figure 1. Coordinate system

The continuity and Euler equations are assumed to govern the fluid flow inside of the tank:

$$\nabla\cdot\vec{u}=0 \qquad \text{and} \qquad \frac{\partial\vec{u}}{\partial t}+\vec{u}\cdot\nabla\vec{u}=-\frac{1}{\rho}\nabla\vec{p}+\vec{f} \tag{2}$$

where $\vec{u}(u,v,w)$ is the velocity vector, defined in the tank-fixed coordinate. Moreover, ρ, p and $\vec{f}$ are the liquid density, pressure and external force vectors, respectively. The external force consists of the gravitational force, translational and rotational inertia forces, which can be written as

$$\vec{f}=[\mathrm{T}(\xi_4,\xi_5,\xi_6)]\cdot\left(\vec{g}-\frac{d^2\vec{\xi}_{1,2,3}}{dt^2}-\frac{d\vec{\Omega}}{dt}\times\vec{r}_G-2\vec{\Omega}\times\frac{d\vec{r}_G}{dt}-\vec{\Omega}\times(\vec{\Omega}\times\vec{r}_G)\right) \tag{3}$$

where $\vec{g}$, $\vec{\xi}_{1,2,3}$ and $\vec{\Omega}$ are the gravitational force vector, the translational motion vectors (ξ_1, ξ_2, ξ_3) and rotational velocity vectors $(\dot{\xi}_4, \dot{\xi}_5, \dot{\xi}_6)$ of the ship motion. [T] is the transform matrix from ship-fixed coordinate to tank-fixed coordinate. In addition, $\vec{r}_G$ is the position vector of the considered point from G. On the free surface, both the kinematic and dynamic conditions should be satisfied.

$$\frac{\partial \eta}{\partial t} + \vec{u} \cdot \nabla \eta = 0 \qquad \text{and} \qquad p = p_{atm} \tag{4}$$

where η indicates the free surface profile and p_{atm} is the air pressure inside of the tank. In addition, a proper wall condition is necessary on the tank walls and internal members. Then the slosh-induced forces and moments on the tank can be obtained by integrating the pressure on the tank surface S_{tank}.

$$\vec{F}_{slosh}(t) = \int_{S_{tank}} p \begin{pmatrix} \vec{n} \\ \vec{r}_G \times \vec{n} \end{pmatrix} dS \tag{5}$$

where $\vec{n}$ is the normal vector on the surface.

The ship motion has been solved using a three-dimensional panel method. Particularly, the Large Amplitude Motion Program (LAMP) program has been used for the time-domain solution. In this computation, the Rankine source has been distributed on the hull surface and local free surface near the body, and the transient wave Green function has been distributed on the matching surface for the radiation condition. The detailed numerical scheme for this mixed-singularity can be found in [3].

The sloshing flow has been solved using the finite difference method described in [2] without viscosity. The key concept of this method is to predict the global fluid motion, and hence some local phenomena have been ignored. This numerical method adopts the SOLA scheme in the fluid domain and SURF scheme for the free surface conditions. The impact pressure on the tank top is also predictable using the scheme introduced in [1] and [2].

3. COMPUTATIONAL RESULTS

The numerical tests have been carried out two models, a modified S175 hull and a VLCC with 17 oil cargo holds. Figure 2 shows the hull form equipped with an ART. The beam(B)-length(L) and draft-length ratios are 0.288 and 0.084, respectively. Bai [4] has reported the experimental data for a supply vessel with the same length characteristics, although the hull forms are not the same. In his experiment, two types of ART, with and without pillars, have been considered. The present computation has been applied for the same size of ART, and its lengths are shown in Figure 3. In this experiment, the five circular pillars have been equipped as shown in the left figure, while the flat plates have been considered in the numerical computation. Only the beam sea condition has been considered for this ship, since the roll motion is of major interest. The linear damping coefficient has been applied for roll motion, and 2.5% of the critical damping has been used in all computation.

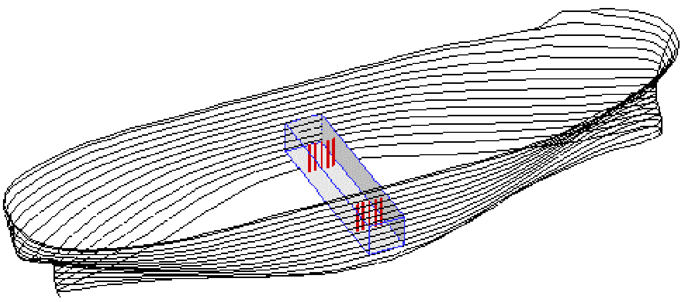

Figure 2. Modified S175 hull equipped with an ART

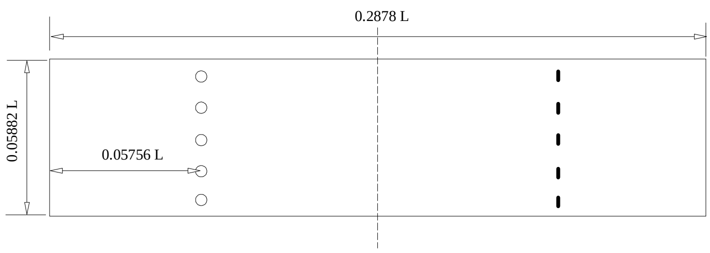

Figure 3. Characteristic lengths of ART with pillars; experimental (left) and computation (right)

The essence of ART design is to tune the ship motion and sloshing flows. That is, the natural frequency of sloshing mode should be well tuned with that of roll motion. Figure 4 shows the time-histories of the wave-induced moment, slosh-induced moment and the resultant roll response. In this case, the filling ratio is 50%. At this filling condition, the natural frequency of fundamental sloshing mode is close to that of the roll motion. From this figure, it can be observed that the phase difference of the wave excitation and slosh-induced moment is close to 180 degrees, resulting in the cancellation of the total roll moment. Therefore, it is obvious that the ART can provide a significant reduction of roll amplitude.

Figure 5 shows the instantaneous ship positions at three time steps with and without ART for the same wave condition to Figure 4. As expected, the reduction of the roll motion is very significant. Therefore, a dramatic change of the roll amplitude can be expected when the tuning of two frequencies is successful.

Figure 6 shows the roll RAOs for two ships, the modified S175 hull for the present computation and the supply vessel that was tested by Bai. Since the hull forms of two ships are not the same, the RAO curves should be compared for not quantities but trend. The RAO curves for the cases with ARTs show a dramatic reduction near the roll natural frequencies, but the roll motion can be larger than the case without an ART at out-of-resonance frequencies. This is because the phase difference of the slosh-induced and wave-induced moments is no longer close to 180 degrees, so that the slosh-induced moment can increase the total roll excitation. From this comparison, we can conclude that the present numerical method provides the correct solution of the coupling problem.

The reduction of the roll amplitude using an ART depends on the wave condition. In the realm of linear theory, the wave-induced excitation is linearly proportional to the wave amplitude. However, the slosh-induced moment varies with a nonlinear manner ([5]). Furthermore, in the random ocean, an ART does not guarantee the dramatic reduction as seen in Figure 5. A good survey about the efficiency of ARTs can be found in [6].

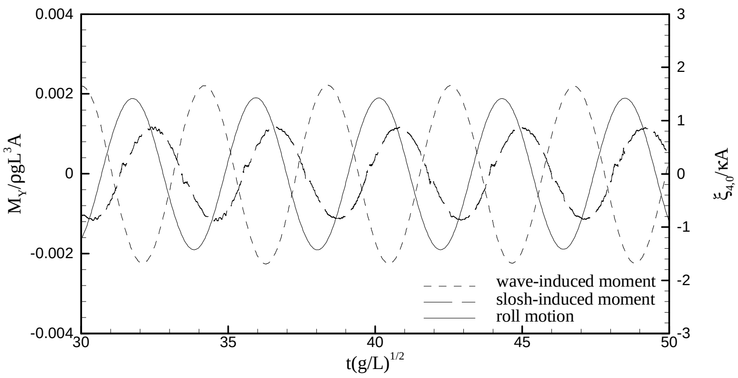

Figure 4. Time-histories of the wave-induced and slosh-induced roll moments; ART without pillars, $\omega\sqrt{L/g}=1.5$, A/L=0.005

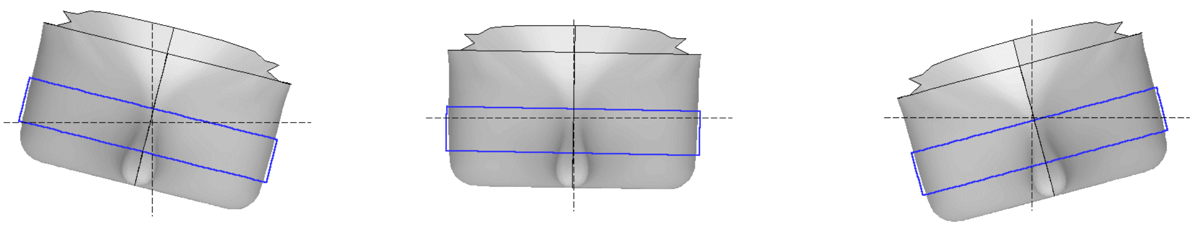

(a) without ART

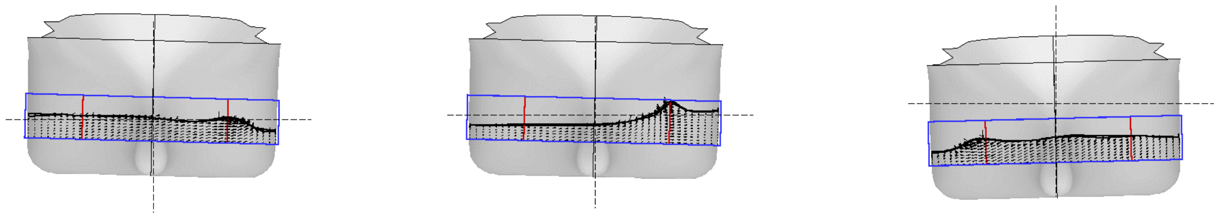

$t\sqrt{g/L}=22.8$ $t\sqrt{g/L}=23.8$ $t\sqrt{g/L}=24.8$

(b) with ART (with pillars)

Figure 5. Instantaneous ship positions and sloshing flows at three time steps; $\omega\sqrt{L/g}=1.5$, A/L=0.05, 50% filling

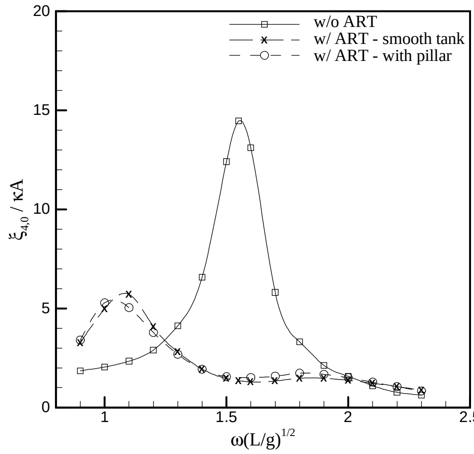

(a) Computational result for modified S175 hull

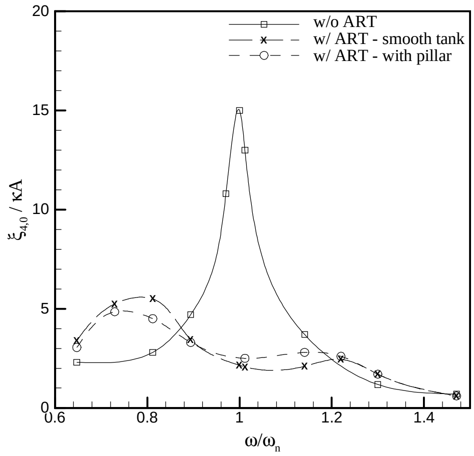

(b) Experimental result for the supply vessel

Figure 6. Motion RAOs of two ships, A/L=0.005

The present method can also be applied to a cargo ship with liquid holds. Figure 7 shows the hull profile (half) and cargo holds for a real ship application. This ship is a typical VLCC of 320-meter long and has 17 oil tanks. Zero speed has been applied, so this ship can be considered as a FPSO also. The center tanks have transverse webs and the wing tanks have

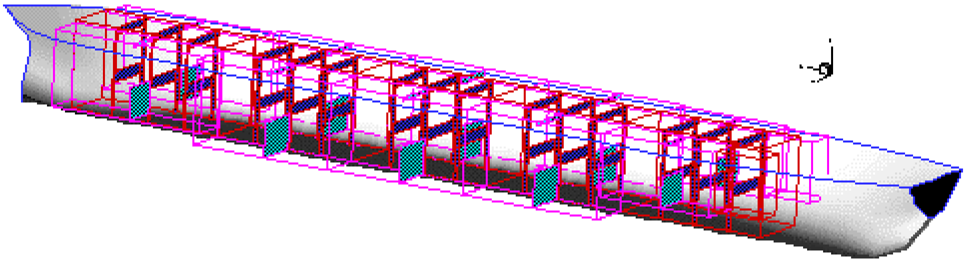

Figure 7. Ship and tank for a real ship computation; 300K VLCC

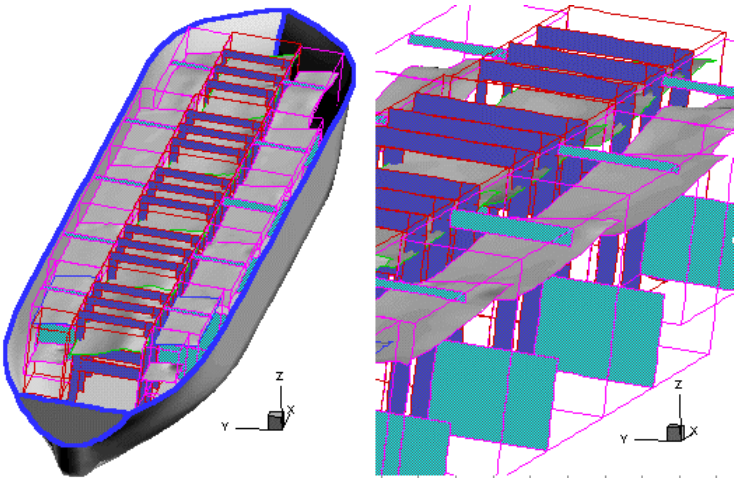

Figure 8. Snapshot of the liquid surface in 17 tanks; 320m VLCC, sea sate 7

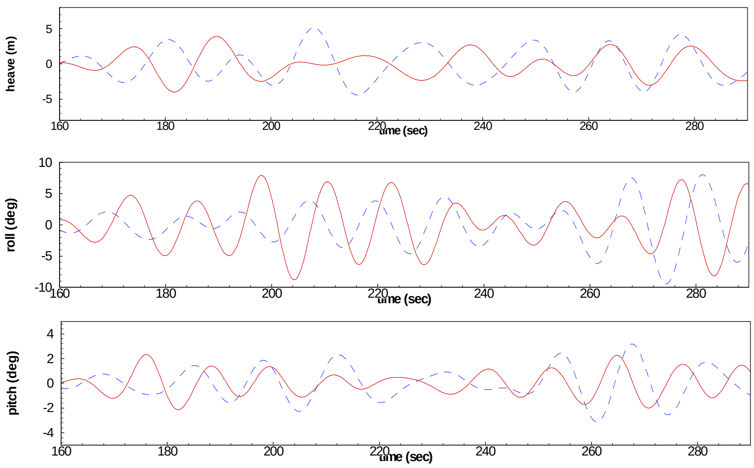

Figure 9. The motion histories at random waves; VLCC, Sea Sate 7, dashed line: without coupling, solid line: with coupling, from above: heave, roll, and pitch

large swash bulkheads at the tank center. In this computation, the random incident waves were applied to excite the freely floating body with zero speed. The modal wave period was 15.0 seconds and significant wave height was 7.5 meters. The filling ratio was fixed to 80% for most tanks. Figure 8 shows an instantaneous snapshot of the liquid profiles inside of the tanks. The corresponding motion histories are in Figure 9. The difference between two motion signals is significant, therefore the coupling effects may play an important role in ships with liquid cargo.

References

[1] KIM, Y., PARK, Y.J., LEE, H.R.: *A numerical study on the prediction of sloshing impact pressure*, Trans. of the Society of Naval Architects of Korea, vol.30 (1994)

[2] KIM, Y.: *Numerical simulation of sloshing flows with impact load*, Applied ocean Research (will appear) (2000)

[3] W.M. LIN et al: *LAMP User's manual*, SAIC (1998)

[4] BAI, K.J., RHEE, K.P.: *Roll-damping tank test*, Seoul National University, Project Report (1987)

[5] VAN DAALEN, E.F.G., GERRITS, J., LOOTS, G.E., VELDMAN, A.E.P.: *Free surface anti-rolling tank simulations with a volume of fluid based Navier-Stokes solver*, Proc. International Workshop on Water Waves and Floating Bodies, Israel, (2000)

[6] MILLER, E.R., SLAGER, J.J., WEBSTER, W.C.: *Phase I report on the development of a technical practice for roll stabilization system selection*, NAVSEC Report 6136-74-280 (1974)